Check for updates

Mild aqueous metal catalyzed oxidative conversion of low-density polyethylene to low molecular weight aliphatic carboxylic acids†

Oleg Davydovich, [iD] [a] Hemant Choudhary, [iD] [b] Daniella V. Martinez,[a] Jay E. Salinas,[a] Estevan J. Martinez,[c] Ryan D. Davis, [iD] [d] Nathan R. Bays,[d] David P. Schafer[d] and Michael S. Kent [iD] *[a]

Aqueous oxidative deconstruction of low-density polyethylene (LDPE) was investigated using homogeneous first-row transition metal catalysts under mild conditions (130–150 °C and ≤100 PSI oxygen pressure). Oxidation of LDPE resulted in high yields of low molecular weight carboxylic acids (up to 75% yield as determined by carbon balance). Aqueous processing is well-suited for biological conversion of the breakdown products.

Commodity plastics have become an integral part of modern society. Due to their low costs and broad applicability, production of plastics continues to grow, approaching 400 million tons (Mt) annually.[1] A significant portion of plastics are used for short-term applications and are immediately discarded after use. Recent studies report that only 9% of discarded plastics are recycled globally; the rest end up in landfills, are incinerated, or are discarded into marine environments.[2] The amount of plastics in landfills and marine environments is expected to reach 12 000 Mt and 150 Mt, respectively, by 2050.[3,4] The majority of plastics in these waste streams are polyolefins (POs) due to their versatility, low cost, and appealing chemical and mechanical properties.[5] While POs such as high-density polyethylene (HDPE), low-density polyethylene (LDPE), and polypropylene (PP) eventually break down in land-based and marine environments, hundreds of years are required to achieve complete degradation.[3]

Efforts to mechanically recycle POs are often inefficient, resulting in materials with substantially reduced mechanical properties, and use processes that release volatile organic compounds.[4,5] The decline in mechanical perfromance

renders the recycled materials useless, leading to their disposal. To advance beyond traditional recycling methods, chemical or biological upcycling of POs has attracted considerable interest for achieving a more circular carbon economy.[6–8] The primary goal is to produce high value monomeric feedstocks, waxes, lubricants, or fuels.[9–14] Due to their stable C–C backbone bond structure, PO chemical conversion is challenging, typically requiring harsh conditions including high temperatures and pressures, toxic metal catalysts, and caustic chemical species. Upcycling polyolefin films is particularly of interest since film products can damage mechanical recycling equipment and thus are generally unwanted by material recovery facilities.[15] Against the backdrop of inefficient mechanical recycling, the demands of harsh conditions for C–C bond cleavage, and pragmatic concerns in industrial processes, we expect that processes for upcycling waste plastics should embrace the principles of green chemistry.[16]

Herein, we report a new method of aqueous metal-catalyzed oxidative deconstruction of LDPE film to produce intermediates suitable for either chemical or biological conversion to value-added products. Earth-abundant and inexpensive first-row transition metal catalysts were utilized to develop a "green" chemical conversion process.[17–19] In prior work, partial oxidation of PE was used to generate low molecular weight polymeric or oligomeric waxes or oils for use as emulsifiers, coatings, inks, additives for textiles, and lubricants.[10,20–24] More extensive deconstruction to low molecular weight oxidized compounds has been demonstrated using dilute aqueous nitric acid with heat[25] or microwave radiation,[26] NO$_x$/O$_2$,[27] permanganate,[20,21,28] aerobic oxidation in acetic acid using metal/bromide[29] or Co(II) and Mn(II) catalysts,[30] Fenton reaction after sulfonation,[31] O$_2$/ozone,[32] and thermal oxidative degradation.[33,34] In the present work, we sought to convert commercial LDPE film into valuable chemicals or precursors (aliphatic carboxylic acids) using mild, aqueous oxidative conditions that do not rely on high temperatures (>150 °C), flammable organic solvents, or caustic/reactive species like nitric acid.[18,19,23,24]

Our initial focus was to survey the effects of various factors, including temperature, metal catalyst type, and catalyst con-

[a]*Department of Environmental System Biology, Sandia National Laboratories, Albuquerque, New Mexico, 87123, USA. E-mail: mmkent88@gmail.com*
[b]*Department of Bioresource and Environmental Security, Sandia National Laboratories, Livermore, California, 94551, USA*
[c]*Department of Organic Materials Science, Sandia National Laboratories, Albuquerque, New Mexico, 87123, USA*
[d]*Department of Materials Reliability, Sandia National Laboratories, Albuquerque, New Mexico, 87123, USA*

centration on the aqueous oxidative deconstruction of LDPE film (30 μm thick, Goodfellow). This film was specifically chosen since it is composed of high molecular weight LDPE (225 000 g mol^{-1}). Higher molecular weight polymers generally require more strenuous deconstruction conditions. Several catalysts were utilized, including KMnO$_4$, CuSO$_4$, CoSO$_4$, and FeSO$_4$ with loadings ranging from 2.5 to 10 weight percent relative to LDPE substrate (Scheme 1). Reactions were carried out in a 1 L T316 stainless steel reactor using a 5 mg mL^{-1} loading of LDPE at 130 °C and 150 °C, and an initial oxygen pressure of 100 PSI (6.9 bar) over the course of 20 h. Oxidation yielded a high fraction of water-soluble products and small amounts of insoluble materials. Reactions at temperatures at or below the melting point of LDPE (110–120 °C) resulted in greatly decreased yields of soluble products and were not studied further. To facilitate the analysis of products, insoluble material was removed by centrifugation. The remaining solution was mixed with a cation exchange resin to remove metal salts (Table S1†), filtered, and freeze-dried (Scheme 1C).

The water-soluble products were first analyzed by elemental analysis to determine the efficiency of each reaction. Fig. 1 and Tables S2 and S3† show the yield for each reaction, quantified as the mole percent of carbon recovered as water-soluble products relative to that in the original LDPE film. Fig. 1 also shows the portion of the carbon in water-insoluble species that did not fully break down and, by difference, the volatile fraction lost during the reaction or upon freeze-drying. Water-insoluble compounds were not characterized by mass spectrometry due to their low abundance and heterogeneity, but size exclusion chromatography (SEC) confirmed they are partially deconstructed (discussed below). The major fraction of
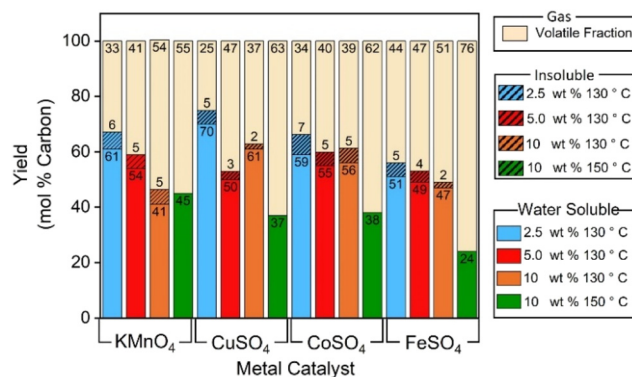

Fig. 1 Carbon recovery after LDPE oxidation using various catalyst concentrations and reaction temperatures. Percent carbon was determined from the carbon recovered in the water soluble and insoluble products using elemental analysis and the carbon content of the initial LDPE film. The mole percent carbon present in volatile moieties was determined as the difference between the carbon of the initial LDPE film and that recovered in water and insoluble soluble products. Catalyst weight percent is calculated relative to LDPE substrate. CoSO$_4$ and FeSO$_4$ are heptahydrate salts.

the oxidized products was water-soluble and accounted for 24–70 mol% of the carbon relative to the pristine LDPE film. Surprisingly, reactions using the lowest catalyst concentrations (2.5 wt% relative to substrate) at 130 °C demonstrated the highest yields. For those reactions, 51–70 mol% carbon was recovered (Fig. 1) which is comparable to previously reported oxidative deconstruction methods.[26,29,30,35] In all cases, except for oxidation using KMnO$_4$, increasing the reaction temperature to 150 °C (at 10 wt% catalyst) resulted in a significant decrease in carbon recovery. This decrease is consistent with Partenheimer's work on metal-catalyzed LDPE autooxidation, which demonstrated a similar reduction in yield when increasing reaction temperature, presumably through over-oxidation resulting in volatile products.[29] We note that stainless steel reactors can catalyze LDPE oxidation, thus several control experiments including no catalyst were performed to establish the catalytic activity of the metal salts used in this study. Reactions without catalyst showed a small amount of conversion (23 ± 2.9 mol% of carbon recovered, Fig. S21†).

Thermally driven polyethylene autooxidation proceeds through an intricate multistep process that imparts oxygen-containing moieties onto the aliphatic backbone, which can be followed by a C–C cleavage event. Prior studies have reported that metal-catalyzed PO autooxidation (in the presence of Co and Mn catalysts) proceeds via a free radical reaction to generate alkyl radicals (postulated mechanism shown in Fig. S1†).[29,36–38] Oxygen reacts with alkyl radicals to generate peroxy radical intermediates. Metal catalyzed homolytic O–O bond cleavage of the peroxide results in the formation of alkoxy radicals which can then undergo C–C bond cleavage via β-scission. Further oxidation results in the formation of carboxylic acid moieties, primarily aliphatic dicarboxylic acids (ADAs) (Scheme 1a); however species containing ketones and
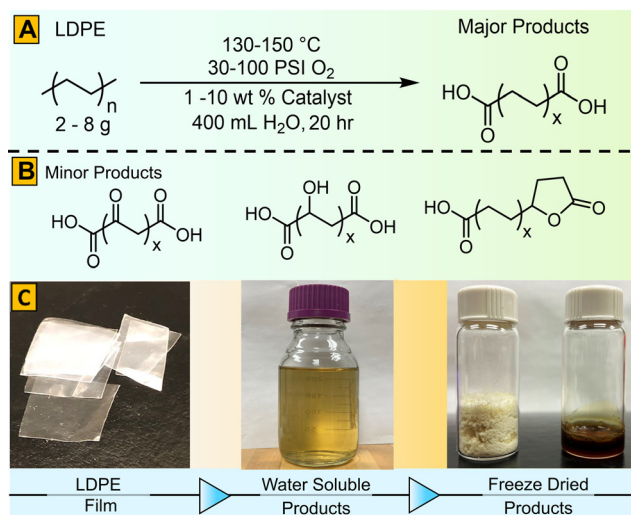
Scheme 1 Metal catalyzed aqueous oxidation of low-density polyethylene (LDPE). (A) Reaction scheme depicting the various conditions used to oxidize LDPE into water-soluble aliphatic dicarboxylic acids. (B) Proposed minor products formed during the reaction. (C) Photographs of the oxidative conversion of LDPE film into water-soluble fragments followed by freeze-drying.

γ-lactones may also be formed.[30,34] While the present work employs individual metal catalysts rather than combinations of Co and Mn catalysts as in the prior work, we posit that a similar autooxidation mechanism occurs. Given their solubility in water, we surmised that the products were likely comprised of significantly deconstructed fragments with hydrophilic groups such as carboxylic acids and hydroxyls. Aqueous SEC shown in Fig. 2 and Fig. S2–S5† demonstrates LDPE deconstruction into low molecular weight compounds ranging from 100–600 gmol^{-1}. Interestingly, the molecular weight range for the deconstructed products was not strongly impacted by reaction temperature and catalyst concentration

(Fig. S2–S5†). The remaining water-insoluble species were characterized by SEC (toluene mobile phase) which indicated partial LDPE deconstruction into compounds with molecular weights ranging from 500–1200 gmol^{-1} (Fig. S6†). However, these products were generally heterogenous and were not always completely recovered from the reactor. Fourier transform infrared spectroscopy (FTIR) was used to identify the various functional groups of the water-soluble products. FTIR spectra shown in Fig. 3 and Fig. S7–S11† reveal the presence of carboxylic acids (1704 cm^{-1}) and carboxylates (1565 cm^{-1}).[39] The peaks shift between the protonated and deprotonated state upon adjusting the pH, as shown in Fig. 3A and Fig. S7–S10.†
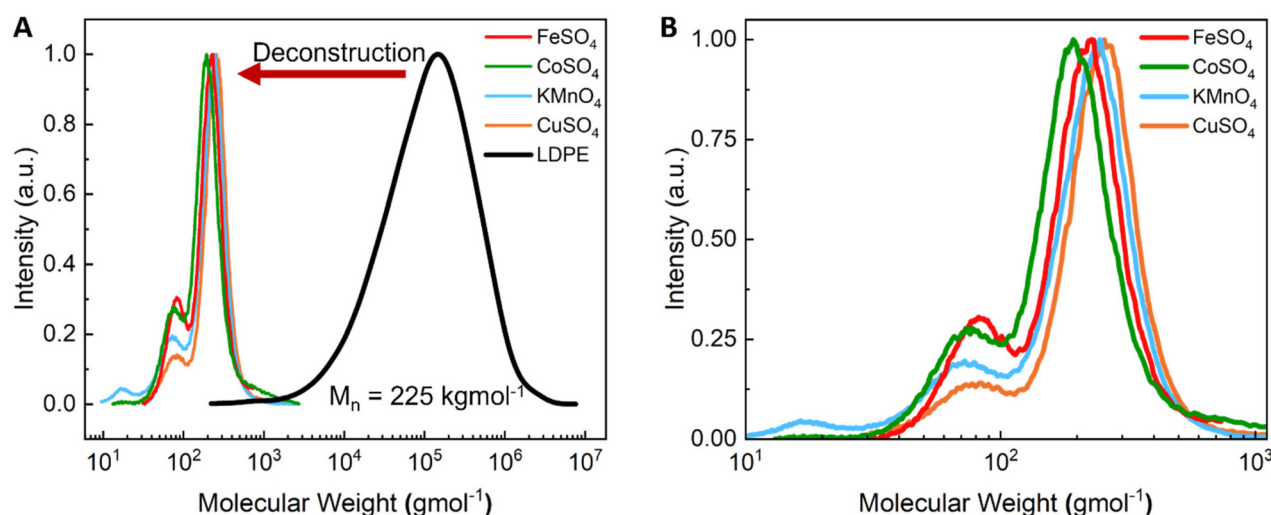

Fig. 2 Representative size exclusion chromatograms of water-soluble oxidized products. (A) Water-soluble products relative to the original film. (B) Expanded view of the lower molecular weight region relevant to deconstructed products. The following reaction conditions were used: 2.5 wt% catalyst loading, 130 °C, and an initial oxygen pressure of 100 PSI.
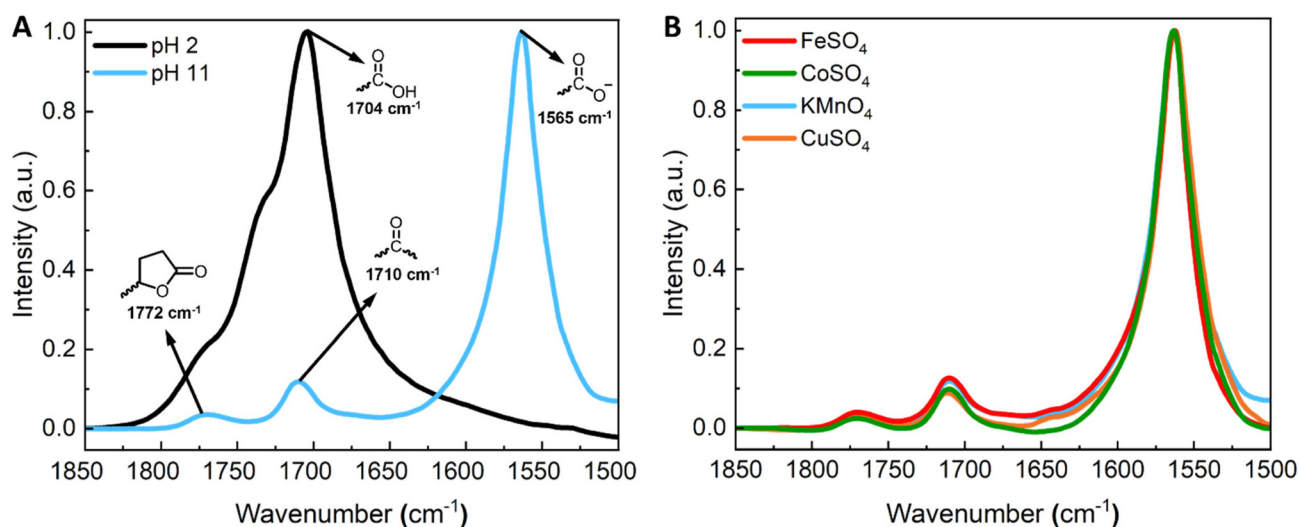

Fig. 3 FTIR spectra of water-soluble oxidized products. (A) FTIR spectra for the water-soluble oxidized products of the reaction with 2.5 wt% KMnO$_4$ at pH 2 and pH 11. (B) Representative FTIR spectra for the water-soluble oxidized products after adjusting pH to 11. Reactions were run using 2.5 wt% catalyst, 130 °C, and an initial oxygen pressure of 100 PSI for 20 h.

pH adjustment from 2 to 11 revealed the presence of small amounts of ketone and γ-lactone species (Fig. 3, 1710 cm^{-1} and 1772 cm^{-1}, respectively).[40]

The deconstructed products were further characterized using high-performance liquid chromatography mass spectrometry (LCMS) and direct injection electrospray ionization high resolution mass spectrometry (ESI-MS). Both techniques show a complex distribution of water-soluble products. LCMS characterization confirmed ADAs as the major products *via* spiking with commercial standards (Fig. S12, see ESI† for details). Direct injection ESI-MS spectra (Fig. S13–S16†) showed the total distribution of products for each reaction that range from 100–400 g mol^{-1}. FeSO$_4$ reactions at 130 °C exhibited increased selectivity for lower molecular weight com-

pounds at a reduced catalyst concentration, whereas CuSO$_4$ and CoSO$_4$ reactions showed opposite trends (Fig. S14 and S15†). On the other hand, oxidation with KMnO$_4$ showed minimal changes in product distributions except for reactions with 10 wt% catalyst at 130 °C which demonstrated a narrower distribution of compounds ranging from 150–250 gmol^{-1} (Fig. S16C and D†). Reactions with Co, Cu, and Fe salts at 150 °C yielded higher amounts of lower molecular weight compounds (Fig. S13D–S15D†). Notably, oxidation with 10 wt% KMnO$_4$ at 150 °C did not significantly alter the distribution relative to reactions at 130 °C (Fig. S16D†).

Having surveyed various catalysts for their ability to oxidatively deconstruct LDPE, we further investigated the most efficient method, utilizing CuSO$_4$, to better understand the
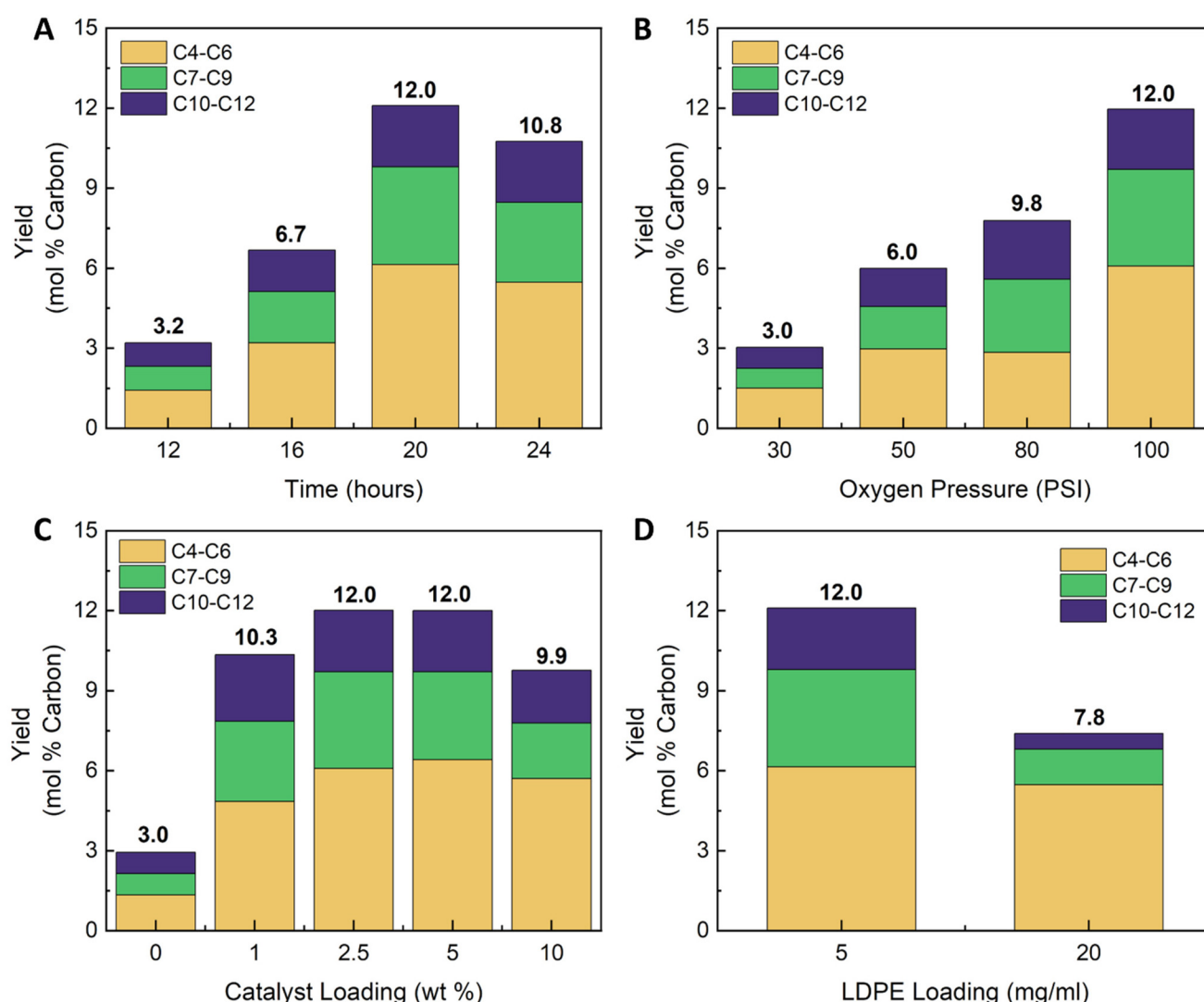

Fig. 4 Aliphatic dicarboxylic acid yield for CuSO$_4$ catalyzed low-density polyethylene oxidation reactions. (A) Time course experiments using 2.5 wt% CuSO$_4$ using an initial oxygen pressure of 100 PSI. (B) Variation in ADA yield with oxygen pressure variation using 2.5 wt% CuSO$_4$, 20 h reaction time. (C) Variation in ADA yield with catalyst concentration using an initial oxygen pressure of 100 PSI and 20 h reaction time. (D) Variation in ADA yield with LDPE loading using an initial oxygen pressure of 100 PSI and 2.5 wt% CuSO$_4$. Temperature was kept constant across all reactions at 130 °C. Yield is determined as the mol% of carbon in the ADA products relative to the LDPE substrate. Legend shows the identity of ADAs based on their carbon chain length.

effects on efficiency and product distribution. Specifically, reaction time, oxygen content (noted as the initial oxygen pressure), catalyst concentration, and substrate loading were varied. Herein, water-soluble compounds were analyzed in the aqueous phase (after filtration and without freeze-drying) and carbon recovery was quantified *via* total dissolved organic carbon measurements (Table S4†). Fig. S17A† shows the recovered carbon yield over the course of 24 h of oxidation. A noticeable induction period, where no water-soluble products are formed, occurs during the first 6 h (<5 mol% water-soluble carbon), a common phenomenon present in other oxidation reactions in absence of an initiator.[34] After this point, the yield of water-soluble products increased and appeared to plateau at 24 h (Fig. S17A,† 75 mol% carbon recovered). Multiple reactions were performed at the same conditions to determine reproducibility (2.5 wt% $CuSO_4$, 100 psi O_2, 130 °C, 20 h) yielding an average of 68 ± 3.8 mol% carbon recovered as soluble species, shown in Fig. S21.† LCMS characterization indicates that the major peaks correspond to ADAs. Fig. 4A shows ADA quantities based on their chain lengths. The major fraction of ADAs was consistently comprised of lower molecular weight compounds (C4–C6). ADA yield consistently increased until the 20 h mark, reaching a maximum of 12 mol%. Oxygen loading (initial oxygen pressure) had a marked impact on both the yield and ADA distribution (Fig. S17B† and Fig. 4B). Presumably, this outcome arises from the increased water solubility of oxygen at higher partial pressures of oxygen, thus increasing the amount of reactive oxidizing species present in the solution.[41] The total carbon yield peaks when using 80 PSI (5.5 bar) of oxygen (Fig. S17B†), whereas the selectivity for ADAs increased consistently up to 100 PSI oxygen (Fig. 4B). Alternatively, the effect of varying catalyst concentration (1–10 wt%) had a nominal effect on the total carbon yield. The highest selectivity for ADAs was attained when using 2.5 and 5 wt% $CuSO_4$ (Fig. 4C). Raising the catalyst concentration resulted in a decrease in total amount of ADA (Fig. 4C) which may be caused by ADA oxidation and conversion into other compounds (Scheme 1C). Increasing the loading of LDPE to 20 mg ml^{-1} resulted in a decrease in the total carbon recovered (51 mol%, Table S3†) and ADA yield (7.8 mol%, Fig. 4D). At higher substrate loadings, some of the ADAs may have precipitated which could explain the reduction in yield. Comparing all the reactions together shows that the total yield of ADAs ranged between 6–12 mol% (Fig. 4), yet the total yield of soluble carbon approached 75 mol% (Fig. S17†). The significant disparity between ADA content and overall yield may stem from oxidation reactions that impart other oxygen functional groups onto the aliphatic backbone. The prominence of carboxylic acid groups in the FTIR data (Fig. S18†) suggests that the non-ADA products are comprised of functionalized low molecular weight aliphatic carboxylic acids. Possible compounds include ADAs functionalized with hydroxyl, carbonyl groups, and aliphatic carboxylic acids bearing γ-lactones (Scheme 1B). Further, substantial carboxylic acid-metal complexes in the product mixture may partially explain the lower yield of ADAs compared to total soluble carbon since metal-
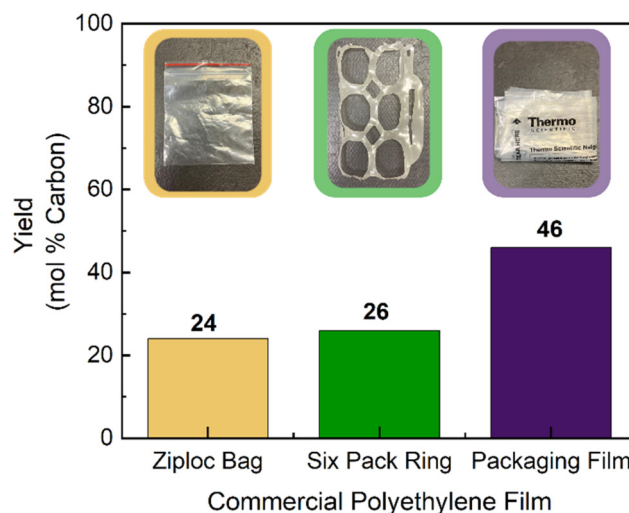

Fig. 5 Carbon recovery after oxidative conversion of post-consumer low-density polyethylene films. Reaction conditions: 5 mg ml^{-1} loading of plastic film, 10 wt% $FeSO_4$, 130 °C, 100 PSI O_2, 20 h. Films include a Ziploc bag, an LDPE six-pack ring, and an LDPE packaging film.

complexed carboxylic acids could not be identified using LCMS.

As a proof of concept, we assessed the broad applicability of this oxidation process by performing oxidation using $FeSO_4$ on other commercial LDPE products including a Ziploc bag, a recycled LDPE six pack ring, and an alternative packaging film (detailed in the ESI†). SEC data shown in Fig. S19† demonstrates successful deconstruction into low molecular weight fragments. The distribution of products by ESI-MS was consistent with the results described above for Goodfellow LDPE film (Fig. S20†). However, the yield of carbon in the water-soluble products was substantially reduced (<30 mol%) in the case of the six-pack holder and Ziploc bag and very little insoluble material was present (Fig. 5). Together, this suggests that the material was overoxidized, resulting in the release of low molecular weight volatile compounds (*i.e.*, CO_2). Overoxidation may arise from the presence of other components in these commercial products that may be more susceptible to the formation of volatile compounds under oxidative conditions (*i.e.*, polypropylene in Ziploc bags). A more in-depth characterization of the various components in each material is required to fully understand the oxidation reaction for these more complex materials.

Conclusions

We developed a mild and efficient method of metal-catalyzed aqueous oxidation to convert LDPE into aliphatic carboxylic acids. Our findings indicate that this deconstruction process results in high carbon recovery (up to 75% carbon recovery) in the form of low molecular weight carboxylic acids as major products. The oxidative process developed in this work serves as an efficient "green" platform to generate valuable feedstocks

for upcycling into useful polymers such as polyamides or polyesters. Utilization of aqueous conditions and a biocompatible catalyst (notably $FeSO_4$) will also allow microbial bioconversion without requiring catalyst removal or other post processing steps. For chemical upgrading, removal of catalyst may be required. We note that the majority of catalyst can be removed with pH-based precipitation, a cation exchange resin, or by reactive distillation which is a common industrial practice for purification of carboxylic acids. Moreover, the use of low-cost and earth-abundant catalysts such as Fe and Cu is promising for scale-up, although a full technoeconomic analysis is required to determine the industrial viability of this method. Since this method cleaves C–C bonds in the backbone of LDPE, we expect it to be broadly applicable in the chemical conversion of other POs such as HDPE and PP.

Author contributions

O. D. and M. S. K. developed the initial project idea. O. D. ran deconstruction experiments, and characterized deconstructed samples using size exclusion and mass spectrometry. D. M. and J. S. helped with deconstruction experiments and with size exclusion chromatography. E. J. M. performed Fourier transform infrared spectroscopy, R. D. D., D. P. S., and N. R. B. helped develop the guidelines for mass spectrometry experiments. H. C. performed large scale reactions and provided valuable discussions. All authors particiapted in writing and editing.

Data availability

The data supporting this article have been included as part of the ESI.†

Conflicts of interest

O. D., H. C., and M. S. K. are named inventors on a related patent application. There are no other conflicts to declare.

Acknowledgements

References

1 Y. Miao, A. von Jouanne and A. Yokochi, *Polymers*, 2021, 449.

2 A. L. Brooks, S. Wang and J. R. Jambeck, *Sci. Adv.*, 2018, **4**, eaat0131.

3 A. Chamas, H. Moon, J. Zheng, Y. Qiu, T. Tabassum, J. H. Jang, M. Abu-Omar, S. L. Scott and S. Suh, *ACS Sustainable Chem. Eng.*, 2020, **8**, 3494–3511.

4 Q. Hou, M. Zhen, H. Qian, Y. Nie, X. Bai, T. Xia, M. L. U. Rehman, Q. Li and M. Ju, *Cell Rep. Phys. Sci.*, 2021, **2**, 100514.

5 D. Jubinville, E. Esmizadeh, S. Saikrishnan, C. Tzoganakis and T. Mekonnen, *Sustainable Mater. Technol.*, 2020, **25**, e00188.

6 A. H. Westlie, E. Y. Chen, C. M. Holland, S. S. Stahl, M. Doyle, S. R. Trenor and K. M. Knauer, *Macromol. Rapid Commun.*, 2022, **43**, e2200492.

7 M. Chu, W. Tu, S. Yang, C. Zhang, Q. Li, Q. Zhang and J. Chen, *SusMat*, 2022, **2**, 161–185.

8 L. D. Ellis, N. A. Rorrer, K. P. Sullivan, M. Otto, J. E. McGeehan, Y. Román-Leshkov, N. Wierckx and G. T. Beckham, *Nat. Catal.*, 2021, **4**, 539–556.

9 P. Patel and A. Tullo, *ACS Discovery Report – The future of plastic*, C&EN, 2020.

10 S. C. Kosloski-Oh, Z. A. Wood, Y. Manjarrez, J. P. de los Rios and M. E. Fieser, *Mater. Horiz.*, 2020, **8**, 1084–1129.

11 J. E. Rorrer, G. T. Beckham and Y. Román-Leshkov, *JACS Au*, 2021, **1**, 8–12.

12 S. Liu, P. A. Kots, B. C. Vance, A. Danielson and D. G. Vlachos, *Sci. Adv.*, 2021, **7**, eabf8283.

13 X. Zhen, E. M. Nuwayo, Z. Qikun, S. Mengqi, P. Carlos, P. Venturo, N. A. Rorrer, J. Miscall, B. G. Sumpter and G. Liu, *Science*, 2023, **381**, 666–671.

14 Y. Miao, Y. Zhao, G. I. N. Waterhouse, R. Shi, L.-Z. Wu and T. Zhang, *Nat. Commun.*, 2023, **14**, 4242.

15 M. A. Martín-Lara, J. A. Moreno, G. Garcia-Garcia, S. Arjandas and M. Calero, *J. Cleaner Prod.*, 2022, **365**, 132625.

16 J. García-Serna, R. Piñero-Hernanz and D. Durán-Martín, *Catal. Today*, 2022, **387**, 237–243.

17 J. R. Ludwig and C. S. Schindler, *Chem*, 2017, **2**, 313–316.

18 R. A. Singer, S. Monfette, D. Bernhardson, S. Tcyrulnikov, A. K. Hubbell and E. C. Hansen, *Org. Process Res. Dev.*, 2021, **25**, 1802–1815.

19 M. Bystrzanowska, P. Petkov and M. Tobiszewski, *ACS Sustainable Chem. Eng.*, 2019, **7**, 18434–18443.

20 J. Zawadiak, A. A. Marek, B. Orlińska and Z. Stec, *J. Appl. Polym. Sci.*, 2010, **118**, 1414–1420.

21 J. Zawadiak, B. Orlinska and A. A. Marek, *J. Appl. Polym. Sci.*, 2013, **127**, 976–981.

22 L. Schuster, A. Hettche, W. Liedy, S. Weiss, L. Ehemann, *US Pat*, 5,064,908, 1991.

23 N. Sharifi-Sanjani and P. Bataille, *Polym.-Plast. Technol. Eng.*, 1999, **38**, 1013–1030.

24 K. Wang, R. Jia, P. Cheng, L. Shi, X. Wang and L. Huang, *Angew. Chem., Int. Ed.*, 2023, **62**, e202301340.

25 L. R. Melby, *Am. Chem. Soc.*, 1978, **11**, 50–56.

26 E. Bäckström, K. Odelius and M. Hakkarainen, *Ind. Eng. Chem. Res.*, 2017, **56**, 14814–14821.

27 A. Pifer and A. Sen, *Angew. Chem., Int. Ed.*, 1998, **37**, 3306–3308.

28 M. W. Guzik, T. Nitkiewicz, M. Wojnarowska, M. Sołtysik, S. T. Kenny, R. P. Babu, M. Best and K. E. O'Connor, *Waste Manage.*, 2021, **135**, 60–69.

29 W. Partenheimer, *Catal. Today*, 2003, **81**, 117–135.

30 K. P. Sullivan, A. Z. Werner, K. Ramirez, L. D. Ellis, J. R. Bussard, B. Black, D. G. Brandnew, F. Bratti, B. L. Buss, X. Dong, S. J. Haugen, M. A. Ingraham, M. O. Konev, W. E. Michener, J. Miscall, I. Pardo, S. P. Woodworth, A. M. Guss, Y. Román-Leshkov, S. S. Stahl and G. T. Beckham, *Science*, 2022, **379**, 207–211.

31 C. Chow, W. Wong, K. Y. Ho, C. Chan and C. Gong, *Chem. – Eur. J.*, 2016, **22**, 9513–9518.

32 I. Radecka, V. Irorere, G. Jiang, D. Hill, C. Williams, G. Adamus, M. Kwiecien, A. A. Marek, J. Zawadiak, B. Johnston and M. Kowalczuk, *Materials*, 2016, **9**, 367.

33 A. B. Bjerre and E. Sorensen, *Ind. Eng. Chem. Res.*, 1994, **33**, 736–739.

34 T. J. Smak, P. de Peinder, J. C. Van der Waal, R. Altink, I. Vollmer and B. M. Weckhuysen, *ChemSusChem*, 2024, **17**, e202301198.

35 J. Y. Yao, Y. W. Wang, T. Muppaneni, R. Shrestha, J. L. Roy and G. D. Figuly, *US Pat*, 10,519,292B2, 2019.

36 F. Gugumus, *Polym. Degrad. Stab.*, 2002, **76**, 329–340.

37 F. Gugumus, *Polym. Degrad. Stab.*, 2006, **91**, 3416–3428.

38 Y. Ahn, G. Roma and X. Colin, *Macromol*, 2022, **55**, 8676–8684.

39 T. Balakrishnan, M.-J. Lee, J. Dey and S.-M. Choi, *CrystEngComm*, 2019, **21**, 4063–4071.

40 R. Yang, Y. Liu, J. Yu and K. Wang, *Polym. Degrad. Stab.*, 2006, **91**, 1651–1657.

41 D. Tromans, *Hydrometallurgy*, 1998, **49**, 327–342.